Fan-Spray Atomizers Analysis through Mathematical Modeling

M. Altimira, A. Rivas, R. Antón, G. Sánchez, J. C. Ramos
Department of Mechanical Engineering – Fluid Flow and Thermal Engineering Chair
Antonio Aranzabal Foundation – University of Navarra
TECNUN - Engineering School (Technology Campus of the University of Navarra)

Abstract
The main objective of this work is to determine the most important design parameters in fan spray atomizers and their effect in the atomization features in order to provide a design tool for nozzle manufacturers. A mathematical model relating the geometry and operating conditions to the characteristics of the spray has been obtained and validated. Three different sub-models have been used in series, so that the results of one model become inputs of the next one, namely multiphase flow simulation, instability and break-up model and maximum entropy model. These have been joined achieving a global model of the whole primary atomization process.

Introduction

Since, at the end of the 19th century, Rayleigh published his work on instability of jets [1], the interest in the atomization process and its implementation in industry has grown enormously.

A lot of numerical and experimental studies concerning the physics of the break-up and the atomization process have been developed [2], but only a few of them tackle the relationship between the atomizer design and the spray features. Manufacturers of fan spray atomizers have a little helpful information [3] to design nozzles fulfilling all the requirements.

This works pretends to create a global model of the atomization process by means of the joint of sub-models, providing a useful design tool with low computational needs.

Problem Description

Fan spray atomizers are used basically in agricultural and painting applications. Its operating principle is such that a liquid sheet is formed as the fluid leaves the nozzle, being its shape closely related to the geometry of the outlet.

In this work three different designs of fan spray atomizers (N_1, N_2, N_3) have been analyzed. All of them are for agricultural use and work at the same normal operating conditions, i.e. pressure of 3 bar and 0.8 l/min of volumetric flow rate. The main differences among them are the shape of the outlet and the internal cross-section transitions.

In order to relate the characteristics of the spray with its inner geometry and the operating conditions three sub-models have been used, each one modeling different features of the atomization process.

Firstly, a model of the single fluid flow that takes place inside the atomizer and the multifluid flow near the outlet has been run to acquire knowledge about turbulence creation in the inner flow and liquid sheet formation and development. Interesting data has been obtained and used in the next sub-model, which tackles the formation and growth of instabilities and the subsequent break-up of the liquid sheet.

* Corresponding author: maltimira@tecnun.es

Values of the break-up length and D_{30} have been calculated and introduced, together with several liquid sheet characteristic parameters from the first sub-model, into a formulation based on the Maximum Entropy Principle that provides droplet size and velocity distributions.

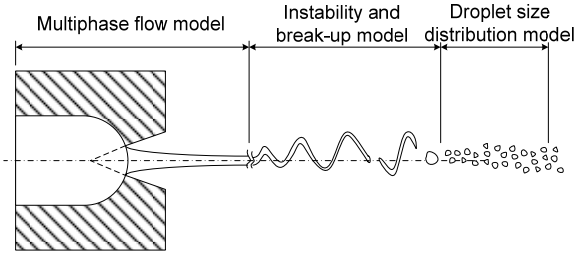

Figure 1: Diagram of the proposed global model

Description of the First sub-model

This sub-model consists on the mathematical modeling of the liquid-gas flow inside and near the outlet of the atomizer. Performance parameters, such as the liquid sheet velocity and thickness, have been obtained and subsequently used as input data in the other sub-models. Other quantities, although they have not been used in following calculations have been included due to their own interest for the designer.

Flow domain

During the first stage of this work, CFD simulations of the inner flow of the nozzles were carried out. Interesting results regarding the creation of turbulence and its influence on the behavior of the liquid sheet were obtained and can be found in [4]. This study concluded that the most characteristic features of the inner flow were developed at the nozzle's tip.

A first attempt was made in [5] to couple the single fluid inner flow and the multiphase outer flow. However, several incongruities were observed in the definition of the boundary conditions. In order to avoid these discrepancies, the domain was extended to include both the tip and the outer geometry of the atomizer. As all the studied designs present two symmetry planes, only a quarter of the whole geometry was modeled.

The dimensions of the domain were chosen in order to observe the complete development of the liquid sheet but not the formation and growth of instabilities or the

break-up, as the mathematical model used is not capable of properly reproducing these phenomena. The dimension perpendicular to the liquid sheet (*Y*) was such that the boundary condition did not affect the liquid flow. Several bidimensional simulations with different values of this magnitude were made in order to check this condition. Additionally, due to the rapidly attenuating sheet thickness, the *Z* dimension was restricted in order to assure a good resolution of the model inside the liquid sheet. Finally, the width of the domain was fixed by its length and the angle of the liquid sheet. The size of the outer domain nondimensionalized with the maximum height of the outlet can be seen in Figure 2.

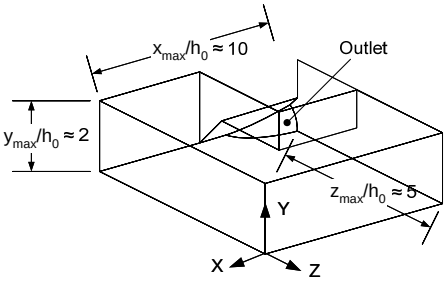

Figure 2: Dimensions of the outer flow domain

Governing equations

The fluids employed in the model are water and air. Water is assumed to be incompressible and the properties of both fluids are considered constant.

The turbulence effects were modeled using the Reynolds Averaged Navier-Stokes (RANS) approach. The RNG *k-ε* model was chosen to close the equations due to its suitability with low Reynolds numbers. Different turbulence models were tested in a bidimensional domain and the values of the magnitudes of interest were proved to be independent of this choice.

Boundary conditions

As previously mentioned, simulations of the atomizer's inner flow were undertaken for different operating pressures [4]. The profiles of total pressure, turbulent kinetic energy and turbulent dissipation rate at the tip inlet were imposed as the inlet boundary condition in the simulations of the extended domain. At the atmosphere boundaries, a zero valued gauge pressure field was set and a no slip condition was enforced at the walls.

Discretization and resolution

The flow domain has been discretized mainly with hexahedral elements, assuring good quality regarding their skewness. The number of elements employed is about three million.

The commercial CFD code Fluent V.6.3, in which the flow governing equations are discretized by means of the Finite Volume Method, has been used to solve the mathematical model.

Governing equations have been discretized using second-order schemes and the SIMPLE algorithm has been chosen for pressure-velocity coupling. An upwind scheme has been used for convective terms, whereas a centered scheme has been adopted for diffusive terms.

To cope with the multiphase flow, the VOF approach [6] has been chosen, as the tracking of the interface was of interest. In this formulation the governing equations are shared by all phases whereas properties like density and viscosity are averaged with the volume fraction of the phases in each cell. Among the different schemes available in Fluent for face flux calculation in VOF, the Euler Implicit has been chosen as the steady solution is wanted. This scheme applies the same interpolation treatment to all cells, regardless of whether they are filled with one phase or more.

Surface tension effects have been considered and introduced into the momentum equation as a source term, according to the continuum surface force (CSF) model developed by Brackbill et al. [7].

Results and discussion

The simulation of the discrete flow domain has provided values of the flow variables such as water volume fraction, velocity, pressure and turbulent quantities. By means of the analysis of these results, interesting integral magnitudes have been obtained, which have been introduced later in the study of instability and break-up of the liquid sheet.

To present the results, a reference frame of cylindrical coordinates has been set with its origin in the point defined by the angle of the liquid sheet and the symmetry plane.

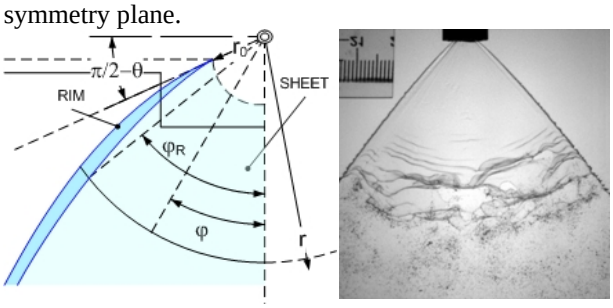

Figure 3: Coordinate System and notation used

For nozzle manufacturers, the knowledge of the spray pattern is essential. Therefore, the angle of the liquid sheet as well as the distribution of mass flow rate as the liquid moves away from the nozzle were measured at different positions.

The nozzle's discharge coefficient, a very important performance parameter in atomization, was calculated according to the following expression:

$$C_D = \dot{V} \cdot P^{-1/2} \qquad (1)$$

being $\dot{V}$ the volumetric flow rate and *P* the working pressure.

Values of the thickness factor *K*, calculated with Eq. (2), have been obtained at different radial coordinates.

$$K = 2h \cdot r \qquad (2)$$

being *h* the local half-width of the liquid sheet.

In Figure 4 the results for N_3 at 3 bar are presented. As can be seen in both curves, the shape of the liquid sheet is closely related to the geometry of the outlet. It is remarkable also the growth of the rim and the fact that the thickness factor has not a constant value throughout the liquid sheet.

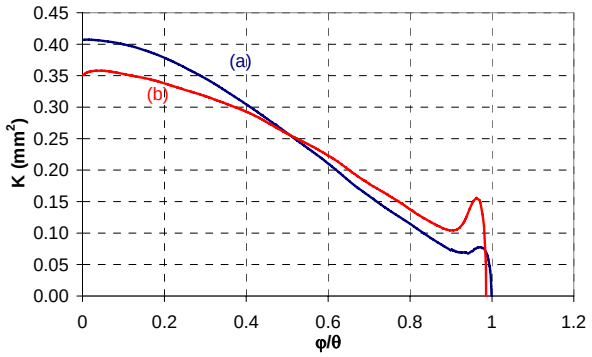

Figure 4: N_3 variation of K with φ (a) Near the outlet (b) Further downstream of the outlet

Magnitudes such as the cross-sectional area, velocity and flow rate have been measured at the sheet neglecting the rim and nondimensionalized with their values at the outlet of the nozzle. The sheet undergoes acceleration near the outlet of the atomizer, increasing its velocity up to 45% depending on the design and the operating conditions. Further downstream it becomes uniform as can be observed in Figure 5. In the results presented in [5], where only the outer domain was considered, the acceleration was of 57%.

Several works dealing with instability models [8] assumed the liquid sheet uniform velocity was the one given by the discharge coefficient, i.e. the outlet average velocity. Presented simulations have revealed that the liquid sheet velocity (U_l), once it is completely developed, is almost 1.5 times the average outlet velocity. This fact was also observed experimentally by Stetler *et al.* [9].

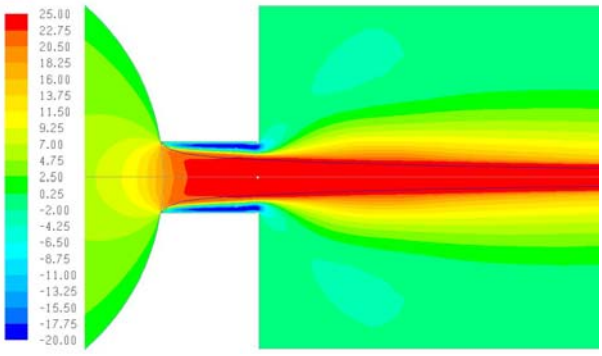

Figure 5: Z velocity (m/s) at the vertical symmetry plane

Description of the Second sub-model

The second sub-model tackles the temporal growth of instabilities and break-up of the liquid sheet. Using the values of the thickness factor and the velocity of the developed liquid sheet from the previous sub-model, a linear instability model has been completed with a simple break-up hypothesis.

The most critical perturbation parameters, i.e. growth rate (ω_r) and wave number (k), and the break-up length (R_B) have been calculated adopting a non viscous attenuating liquid sheet and, hence, calculating the Weber number with the local width of the sheet as characteristic length. The inviscid assumption is based on the low values of the Ohnesorge number present through the range of operating conditions.

The nondimensional dispersion relation used is the one derived by Squire [10] and Hagerty and Shea [11] for a bidimensional inviscid liquid sheet, where the perturbation growth rate is given by

$$\tilde{\omega}_r = \frac{m}{\rho + \tanh(m)}\left\{We_g \cdot \tanh(m) - m\left[\rho + \tanh(m)\right]\right\}^{\frac{1}{2}} \quad (3)$$

being the nondimensional numbers

$$\tilde{\omega}_r = \omega_r \cdot \left(\sigma / \rho_l \cdot h^3\right)^{-1/2} \quad (4)$$

$$m = k \cdot h \quad (5)$$

$$We_g = \frac{\rho_g \cdot U_l^2 \cdot h}{\sigma} \quad (6)$$

$$\rho = \frac{\rho_g}{\rho_l} \quad (7)$$

To get the most unstable perturbation, the wave number with the maximum growth rate needs to be numerically calculated solving

$$\frac{\partial \tilde{\omega}_r}{\partial k} = 0 \quad (8)$$

However, other authors made more simplifications to this dispersion relation in order to obtain an expression with an analytical solution. These simplifications have been proved by these workers to give a shorter break-up length than the one given by the complete dispersion relation in an attenuating liquid sheet, as will be seen later.

Although it has been demonstrated that the break-up of a liquid sheet is governed by non-linear effects, using information from the linear instability model in a simple break-up model it is possible to estimate values of the break-up length as well as the size of the droplets formed by the primary atomization.

The break-up model adopted in this work is the one proposed by Dombrowski *et al.* [8]. It assumes the amplitude of the perturbations (η) grow until they reach a certain amplitude, and then break into pieces of length equal to the perturbation wavelength in case of antisymmetrical waves and half the perturbation wavelength in case of symmetrical waves. The distance traveled by the liquid before reaching the break-up condition is defined as the break-up length (R_B) and can be calculated with Eq(9).

$$Ln\left(\frac{\eta}{\eta_0}\right) = \frac{1}{U_l}\int_0^{R_B/U_l} \omega_r \cdot dt = 12 \quad (9)$$

Separated pieces contract forming ligaments which, according to the expression derived by Rayleigh, collapse into droplets of diameter given by Eq (10)

$$d_D = C \cdot \left(\lambda_B^* \cdot h_B^*\right)^{1/2} \quad (10)$$

being λ_B^* and h_B^* the perturbation wavelength and the half-width at break-up.

The value of constant C needs to be adjusted with experimental data depending on the kind of atomizer. The droplet diameter obtained is the Mass-mean diameter D_{30}, which is necessary to develop the Maximum Entropy model.

Description of the Third sub-model

In spray modeling, having information about droplet size and velocity distribution is very important, since it determines the validity of the spray for a certain application.

Droplet size and velocity distributions can be determined in an experimental or analytical manner. The main drawback of the former is its strong dependence on the type of atomizer. In the latter group, the Maximum Entropy Principle has been proved recently by several works to give accurate results. A clear review about the available methods can be found in [12].

This method was used first in spray drop formation by Sellens & Brzustowski [13], [14] and Li & Tankin [15] assuming the most likely distribution is the one which maximizes the entropy subject to the restrictions imposed by the physical system, as well as the normalization equation. The restrictions used in this work are those from the equations of mass, momentum and energy conservation.

$$\int_{\psi} f \cdot \frac{\pi}{6} D^3 \cdot \rho \cdot \dot{n} \cdot d\psi = \dot{m}_l + S_m \qquad (13)$$

$$\int_{\psi} f \cdot \frac{\pi}{6} D^3 \cdot \rho \cdot \dot{n} \cdot U \cdot d\psi = \dot{m}_l \cdot U_l + S_{mv} \qquad (14)$$

$$\int_{\psi} f \cdot \left(\frac{1}{2} \cdot \frac{\pi}{6} D^3 \cdot \rho \cdot \dot{n} \cdot U^2 + \sigma \cdot \pi \cdot D^2 \cdot \dot{n} \right) \cdot d\psi = \frac{1}{2} \cdot \dot{m}_l \cdot U_l^2 + S_e \qquad (15)$$

$$\int_{\psi} f \cdot d\psi = 1 \qquad (16)$$

$$d\psi = dD \cdot dU \qquad (17)$$

being f the probability density function, $\dot{n}$ the number of droplets formed per unit time, $\dot{m}_l$ the mass flow rate at the exit of the nozzle, S_m the source term that represents the mass transference between both phases, S_{mv} is the source term of momentum corresponding to the drag force that the gas exerts on the liquid phase and S_e representing the transformation of kinetic energy into superficial energy.

Taking the diameter D_{30} and the velocity of the liquid sheet U_l as characteristic magnitudes of the problem, these equations can be nondimensionalized and the probability density function results

$$f = f_0 \cdot \exp\left[-\lambda_0 - \lambda_1 \overline{D}^3 - \lambda_2 \overline{D}^3 \overline{U} - \lambda_3 \left(\overline{D}^3 \overline{U}^2 + \frac{12 \overline{D}^2}{We_{30}} \right) \right] \qquad (19)$$

being

$$We_{30} = \frac{\rho \cdot D_{30} \cdot U_l^2}{\sigma} \qquad (18)$$

λ_i the Lagrange multipliers and f_0 the prior distribution as defined in [17].

The source terms S_m, S_{mv} and S_e are the link between the break-up deterministic model and the primary atomization stochastic model. Assuming there is no evaporation of the liquid, the dimensionless mass source term is zero. A first approximation was made by taking also the momentum and energy source terms as zero.

The optimization problem given by the three conservation equations is solved using a Newton-Raphson Method. Due to the sensitivity of the problem regarding the initial values of the Lagrange multipliers, λ_0 is calculated after each iteration by means of the normalization equation.

Experimental validation

Discharge coefficient

Experimental values of the discharge coefficient were measured at different operating pressures in five units of each studied design.

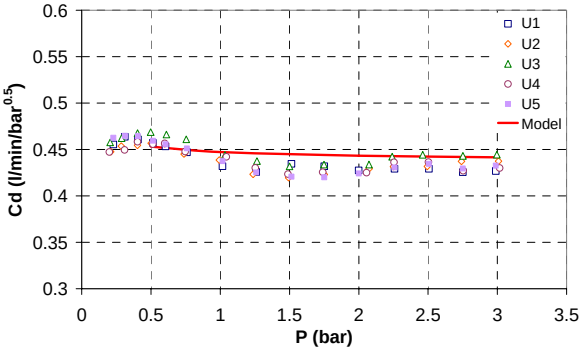

Figure 6: Experimental vs. Simulated values for the Discharge coefficient of N_2

Variations of this parameter of 4% have been observed among units of N_1. In designs N_1 and N_3 differences between experimental and simulated values are up to 15% at low pressures and lower to 5% as the pressure increases, whereas for N_2 are less than 5% for all the range of conditions.

Thickness factor

To measure the sheet thickness factor an interferometric technique proposed by Dombrowsky [16], and later used in other research works [18], which consists in illuminating the liquid sheet with a monochromatic light beam, has been used. Due to the sheet's attenuating thickness, a pattern of constructive and destructive interference is formed. Measuring the distance between two bright fringes and counting the number of intervals between them it is possible to calculate the sheet's thickness factor with the following expression:

$$K = \frac{\lambda}{2n \cdot \cos\beta} \cdot \frac{q - t}{\frac{1}{r_t} - \frac{1}{r_q}} \qquad (20)$$

being λ the light beam wavelength, n the refractive index, β the refraction angle of the light in the sheet and r_q and r_t the radial coordinates corresponding to the q^{th} and t^{th} intervals.

However, the appearance of turbulence makes impossible the formation of the mentioned pattern, as noticed by Fraser et al. [19]. Thus only the values of this parameter corresponding to low operating pressures have been measured. Only for nozzles of model N_1 it was possible to get values of K in a wide range of operating pressures, due to its low turbulence level. For each pressure, the thickness factor was calculated at

three different angular positions, namely: left, right and center of the liquid sheet. Despite the dispersion of the measurements, the results provide a 10% error prediction at the center of the liquid sheet.

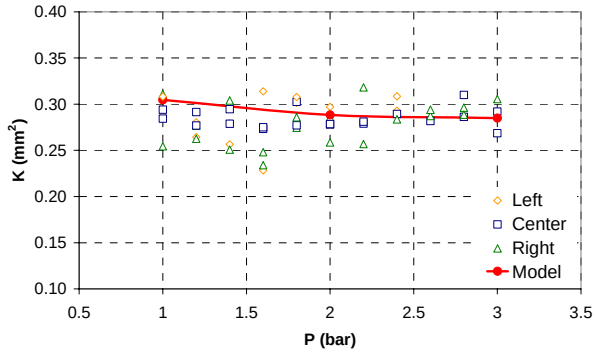

Figure 7: Thickness factor values from the first sub-model and experimental values for N_1

Liquid sheet angle

The liquid sheet angle measured over images shows good agreement with the values obtained from the simulations as can be seen in Table 1.

Table 1: Angles from experimental data and CFD simulations

	N_1	N_2	N_3
θ_{exp} (deg)	92	82	119.7
θ_{sim} (deg)	90	96	114

Flow distribution

The angular distribution of the flow was measured with a patternator and compared with the values obtained from simulations. As can be seen in Figure 8, the pattern predicted for N_3 has good correspondence with the experimental results, although the last ones present a slight asymmetry. The adjustment of the sheet border is worse, due to the absence of rim in the real sheet.

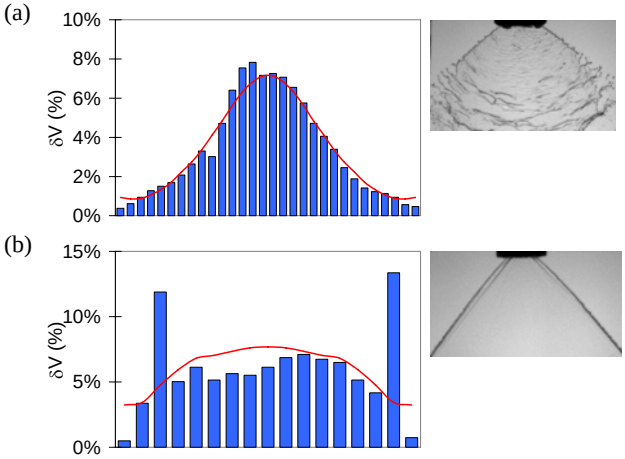

Figure 8: Flow pattern at 3 bar of (a) design N_3 (b) design N_1

On the contrary, the results for N_1 show a noticeable lack of fit at the rim. Seizing on the knowledge acquired it can be concluded that, when the rim does not play an important role in the development of the liquid sheet, CFD techniques provide accurate data of the spray pattern. Whereas, in cases where the rim is formed and even detaches from the sheet behaving like a jet, it is not possible to predict the final flow distribution with the considered domain.

Break-up length

Values of the break-up length were obtained using a High Speed Imaging system and compared with those given by the expression from Dombrowsky and the ones from the integration of the dispersion relation.

It can be observed in Figure 10 that both models fit the experimental values at high Weber numbers. However, at low values of this parameter, none of them is capable of giving accurate results, due to the different break-up process that takes place at low operating pressures. The characteristic length used to nondimensionalize R_B and to calculate the Weber number is the square root of the sheet thickness factor. Similar results were obtained for N_2, whereas for N_1 errors were up to 30% along the high Weber number range.

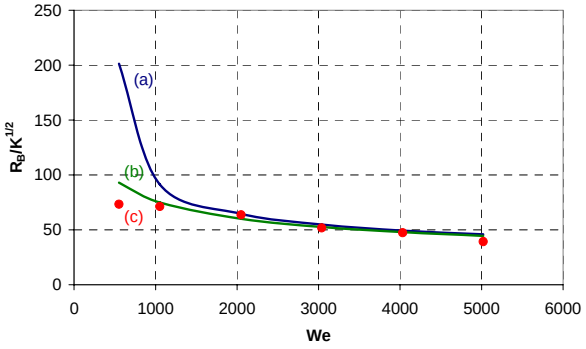

Figure 9: Dimensionless break-up length for N_3 given by: (a) integration of the dispersion relation (b) Dombrowsky expression and (c) experimental values

Droplet size

Droplet size distributions have been obtained experimentally with a Malvern Spraytec sizing system. High data dispersion was observed, up to 30% among the measurements made in the same point and 80% within the entire break-up zone. However, this dispersion is reduced significantly as the operating pressure increases.

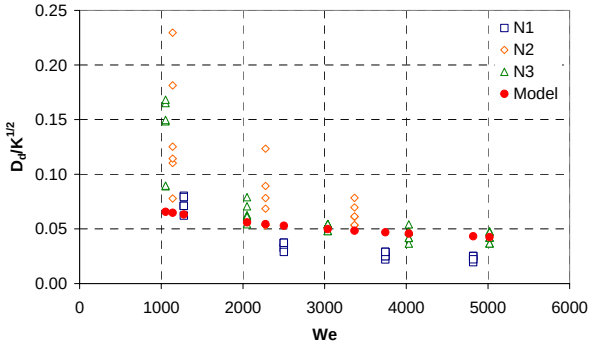

Figure 10: Dimensionless values of D_{30}

Considering only D_{30} from tests with pressure higher than 1 bar, the constant C of equation (10) was adjusted to a value of 0.283.

Calculations of the droplet size distribution with the Maximum Entropy method have not yielded good results, providing a narrower distribution than the one given by the Malvern, with the same D_{30} but lower D_{32} and D_{43}.

Conclusions

Carrying out this work has lead to several conclusions concerning the suitability of the proposed model.

Firstly, it has revealed the fact that at low pressures there is a development of phenomena that the presented model cannot predict and have major influence in primary atomization, as can be seen in the experimental values of the thickness factor, break-up length and D_{30}.

The first sub-model has been proved to be an appropriate and robust tool for nozzle design, not only to obtain important features of the liquid sheet but also as a support of other complementary models such as the break-up and droplet formation models. It has given accurate values of the liquid sheet thickness factor in cases with low turbulence levels. However, due to the basis of the experimental device used, it has not been possible to determine its validity with turbulent flows. The discharge coefficient has been found to be very sensitive to the inner dimensions of the nozzle, presenting significant variations among different units of the same model. The analysis of the flow has concluded that the mean velocity of the developed liquid sheet cannot be calculated through the discharge coefficient, which opposes the assumption made in several works.

For an attenuating inviscid liquid sheet, the integration of the dispersion relation along the liquid sheet, although has given correct values of the break-up length, has not been proved to be more accurate than the simplified expression derived by Dombrowsky due to the liquid sheet behavior at low pressures.

The Maximum Entropy-based sub-model should be completed with a proper representation of momentum and energy changes. Additionally, droplet size distribution should be measured experimentally with a diameter-based device instead of a volume-based in order to avoid numerical errors.

Acknowledgements

This research was carried out with the support of Eusko Jaurlaritza – Gobierno Vasco (Spain) through the project PI2007-13. The authors would like to thank the financial support of Cátedra Fundación Antonio Aranzábal – Universidad de Navarra.

References

[1] L. Rayleigh, On the instability of jets, *Proceedings of the London Mathematical Society*, vol. 10, pp. 4-13, 1878.

[2] W.A. Sirignano, C. Mehring, Review of theory of distortion and disintegration of liquid streams. *Prog. Energy Combust. Sci.*, vol. 26, pp. 609-655, 2000.

[3] Q. Zhou, P.C.H. Miller, P.J. Walklate, N.H. Thomas, Prediction of spray angle from flat fan nozzles, *J. Agr. Eng. Res.*, vol. 64, pp. 139-148, 1996.

[4] A. Rivas, G. Sánchez, A. Estévez, J.C. Ramos, Improving the design of fan spray atomizers through Computational Fluid Dynamics Techniques, *20th ILASS – Europe Meeting*, 2005.

[5] A. Rivas, M. Altimira, G. Sánchez, J.C. Ramos, Analysis of liquid-gas flow near a fan-spray nozzle outlet, *CMFF'06*, 2006.

[6] C.W. Hirt, B.D. Nichols, Volume of Fluid (VOF) Method for the dynamics of free boundaries, *J. Comput. Phys.*, vol. 39, pp. 201-225, 1981.

[7] J.U. Brackbill, D.B. Kothe, and C. Zemach, "A Continuum Method for Modeling Surface Tension", *J. Comput. Phys.*, vol. 100, pp.335-354, 1992.

[8] N. Dombrowski, P.C. Hooper, The effect of ambient density on drop formation in sprays,. *Chem. Eng. Sci.*, vol. 17, pp. 291-305, 1962.

[9] M. Stetler, G. Brenn and F. Durst, "The influence of viscoelastic fluid on spray formation from flat-fan and pressure-swirl atomizers", *Atom. Sprays*, vol. 12, pp. 299-327, 2002.

[10] H.B. Squire, Investigation of the instability of a moving liquid film, *J. Appl. Phys.*, vol. 4, pp. 167-169, 1953.

[11] W.W. Hagerty, J.F. Shea, A study of the stability of plane fluid sheets. *J. Applied Mechanics*, pp. 509-514, 1955.

[12] E. Babinsky, P.E. Sojka, Modeling drop size distributions. *Prog. Energy Combust. Sci.*, vol. 28, pp. 303-329, 2002.

[13] R.W. Sellens, T.A. Brzustowski, A prediction of the drop size distribution in a spray from first principles. *Atomization and spray technology*, vol. 1, pp. 89-102, 1985.

[14] R.W. Sellens, T.A. Brzustowski, A simplified prediction of droplet velocity distributions in a spray. *Combust. Flame*, vol. 65, pp. 273-279, 1986.

[15] X. Li, R.S. Tankin, Droplet Size Distribution: a derivation of a Nukiyama-Tanasawa type distribution function, *Combust. Sci. Technol.*, vol. 55, pp. 65-76, 1988.

[16] N. Dombrowski, D. Hasson, and D.E. Ward, Some Aspects of liquid flow through fan spray nozzles. *Chem. Eng. Sci.*, vol. 12 pp. 35-50, 1960.

[17] S.K. Mitra, Breakup process of plane liquid sheets and prediction of initial droplet size and velocity distributions in sprays. PhD thesis, University of Waterloo, 2001.

[18] Y.J. Choo, B.S. Kang, "Parametric study on impinging-jet liquid sheet thickness distribution using an interferometric method", *Exp. Fluids*, vol. 31, pp. 56-62, 2001.

[19] R.P. Fraser et al., Drop formation from rapidly moving liquid sheets. *A.I.Ch.E. Journal*, vol. 8, pp. 672-680, 1962.